

Electrochemical Performance of Doped SnO₂ Coating on Ti Base as Electrooxidation Anode

Haiqing Xu^{*}, Aiping Li and Xiaochun Cheng

Key Laboratory for Attapulgite Science and Applied Technology of Jingsu Province, Huaiyin Institute of Technology, Huaian, 223003, China

*E-mail: xhqsejs@163.com

Received: 29 August 2011 / Accepted: 11 October 2011 / Published: 1 November 2011

The performance of electrode for the electrochemical treatment of organic contaminants was improved using Ce-doped Ti/SnO₂-Sb electrodes prepared by a thermal deposition method. Cyclic voltammetry (CV) and Amperometric *i*-t Curve were measured showing an improvement of electrochemical feature for the Ti/SnO₂-Sb-Ce electrode. The electrochemical oxidation performance of the prepared electrode was investigated using aniline as a model pollutant. The aniline removal of 98.3% was achieved with the Ti/SnO₂-Sb-Ce electrode after 2 h electrolysis while it was only 82.7% for the Ti/SnO₂-Sb electrode. The removal of chemical oxygen demand (COD) was 80.5% on the Ti/SnO₂-Sb-Ce electrode which was also higher than that on the Ti/SnO₂-Sb electrode (58.4%). The electrode was characterized by scanning electron microscopy (SEM), X-ray diffraction (XRD), electron dispersive spectrometry (EDS), and X-ray photoelectron spectroscopy (XPS). The results show that the coating had larger surface area and higher active O_{ads} content due to Ce doping, which could provide with more active sites for electrochemical oxidation of organic pollutants.

Keywords: Ti/SnO₂-Sb-Ce electrode; Coating; Electrochemical oxidation; Wastewater treatment

1. INTRODUCTION

Industrial wastewaters containing some recalcitrant organic contaminants, such as aromatic hydrocarbons, phenolic compounds and pesticides, due to their toxicity and difficulty to be degraded, becomes intractable problem to environment and potential hazard towards humans and animals health [1,2]. Many technologies have been employed in treatment processes of industrial wastewaters [3-6]. Recently, electrochemical oxidation is becoming a preferable alternative because of its strong oxidation performance, non-selective oxidation and environmental compatibility [7-11]. Organic contaminants can be destroyed electrochemically and effectively degraded to CO₂ or aliphatic products. Research into electrochemical methods for the treatment of organic contaminants has

focused on anodes with excellent oxidation performance. The electrochemical characteristics of the anode are mainly related to the material and structure of the coating. In the past years, numerous types of metal oxide electrodes, such as SnO_2 , PbO_2 and composite oxides, have been developed for electrochemical oxidation of organic pollutants [12-17]. It is well known that doping for these oxides coating will achieve better electrochemical activity [18-20].

Rare earth elements have been proved to enhance catalytic performance by either acting as a catalyst or assisting catalytic processes [21,22]. In electrochemical processes, the doping of rare earth into the film could improve the surface structure and enhance the electrode capability on mineralization of pollutant compounds. It is worthy of mention that the Ce species are active and inexpensive material and are widely used [23]. Recent studies indicate that a better performance is obtained for co-doped electrodes. In this work, we selected rare earth Ce as co-dopant to introduce into $\text{Ti/SnO}_2\text{-Sb}$ by thermal decomposition and examined electrochemical properties of the $\text{Ti/SnO}_2\text{-Sb-Ce}$ electrode.

2. EXPERIMENTAL

2.1. Electrode coating preparation

The electrode coatings were prepared using thermal decomposition technique. Titanium plates ($4.0\text{ cm} \times 4.0\text{ cm} \times 0.1\text{ cm}$) were introduced as the base metal for all oxide-coated electrodes. The Ti substrates were polished using sand papers, treated in 10 % boiling oxalic acid for 2 h and washed. The metal precursors were prepared using the following metal salt compounds: $\text{SnCl}_4 \cdot 5\text{H}_2\text{O}$, SbCl_3 and $\text{Ce}(\text{NO}_3)_3$, with Sn:Sb:Ce (molar ratio 100:6:3) for the $\text{Ti/SnO}_2\text{-Sb-Ce}$ and Sn:Sb (molar ratio 100:6) for the $\text{Ti/SnO}_2\text{-Sb}$. The precursor solutions were obtained by dissolution of citric acid in 5 ml ethylene glycol and 30 ml ethanol mixing solution. The metal precursor was added and kept under ultrasonic dissolution. The molar ratio of the metal: citric acid: ethylene glycol was 1:3:3. The precursor solution was spread on Ti substrate, and then dried for solvent evaporation in an infrared oven at $60\text{ }^\circ\text{C}$ for 30 min, and fired in a muffle oven under air at a temperature of $550\text{ }^\circ\text{C}$ for 15 min. This procedure (spreading, drying and pyrolysis) was repeated 10 times and finally, the electrodes were heated at $550\text{ }^\circ\text{C}$ for 3 h.

2.2. Electrochemical measurement

The coatings of the electrodes were measured by means of CV and Amperometric *i-t* Curve to evaluate the electrochemical performance. All electrochemical measurements were carried out with a Zahner IM6ex electrochemical station using a three-electrode system. $\text{Ti/SnO}_2\text{-Sb-Ce}$ and $\text{Ti/SnO}_2\text{-Sb}$ were used as the working electrode, respectively. Ti plate was used as an auxiliary electrode, and the saturated calomel electrode (SCE) was used as a reference electrode.

2.3. Electrochemical oxidation

The fabricated electrode was used as an anode and a Ti plate with the same area as a cathode, and the distance between the anode and cathode was 15 mm. 100 ml synthetic wastewater was charged in an electrolysis cell. The concentration of aniline was monitored by HPLC during electrochemical oxidation process, which was carried out on a Perkin Elmer Series 200 LC. Chromatographic separation was performed using an ODS-18 reversed phase column. The mobile phase consisted of methanol/water (40/60, v/v) at a flow rate of 1 mL min⁻¹, and 15 µL of sample was injected. The UV detector was set at 275 nm. The COD of the electrolyte was determined using the standard dichromate method (China GB11914-89). The instantaneous current efficiency (ICE) for the anodic oxidation of phenol has been calculated from the values of COD using the following relation [24]:

$$\text{ICE}(\%) = \frac{(\text{COD}_t - \text{COD}_{t+\Delta t})}{8It} FV \quad (1)$$

where (COD)_t and (COD)_{t+Δt} are the chemical oxygen demands at times *t* and *t+Δt* (in g dm⁻³), respectively, *I* is the current (A), *F* is the Faraday constant (96487 C mol⁻¹), *V* is the volume of electrolyte (dm³) and 8 is the equivalent mass of oxygen (g eq⁻¹).

2.4. Characterization of coating

The morphology of the electrode coating was characterized using a SEM (FEI Sirion 200) equipped with an EDS. XRD patterns were used for the crystalline structure identification of the samples and obtained using a D-MAX 2200 VPC instrument with Cu Kα radiation. XPS measurements of the coatings were performed on a PHI 5000 (ULVAC-PHI) system with an Al Kα source. All the binding energies were referenced to the C1s peak at 284.6 eV from the surface adventitious carbon.

3. RESULTS AND DISCUSSION

3.1. Electrochemical measurement

CV was used to evaluate electrochemical performance of the electrode surface. Fig. 1 shows the voltammograms of the Ti/SnO₂-Sb-Ce and Ti/SnO₂-Sb electrodes in 0.1 M KCl solution containing 5 mM K₄[Fe(CN)₆]. CVs were recorded between -0.2 V and 0.6 V vs SCE, and covered the potential region before the beginning of oxygen evolution reaction (OER, 1.6 V vs SCE). In this potential region the observed voltammetric current is the sum of the electrode surface redox transitions and the double layer charging [25]. The CVs displays a pair of the peaks of Fe(CN)₆^{3-/4-} redox, and also showed quasi-reversible processes. Oxidation current peak and deoxidization current peak corresponding to Fe(CN)₆^{3-/4-} redox transition are observed at about 0.34 V and 0.09 V versus SCE, respectively. The

scan curve of Fig. 1a shows a higher current peak of redox transition, indicating that the Ce-doped coating effectively enhances the electron transfer from ferricyanide to the electrode. Integration of the i - E curve provides the voltammetric charge, which is proportional to the number of electrochemically surface active sites [26]. CV scans showed that the voltammetric charge on the Ti/SnO₂-Sb-Ce electrode was more than that on the Ti/SnO₂-Sb electrode, which is attributed to the increase of whole active surface of the Ti/SnO₂-Sb-Ce electrode.

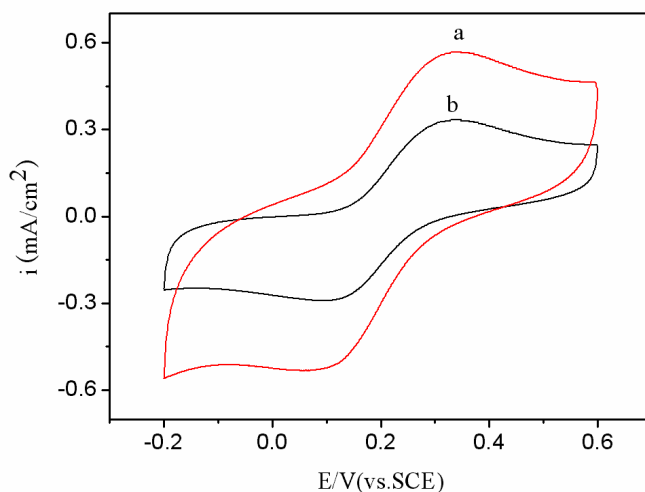


Figure 1. CVs obtained with the Ti/SnO₂-Sb-Ce electrode (a) and the Ti/SnO₂-Sb electrode (b) in 0.1 M KCl solution containing 5 mM K₄[Fe(CN)₆] at a scan rate of 100 mV/s

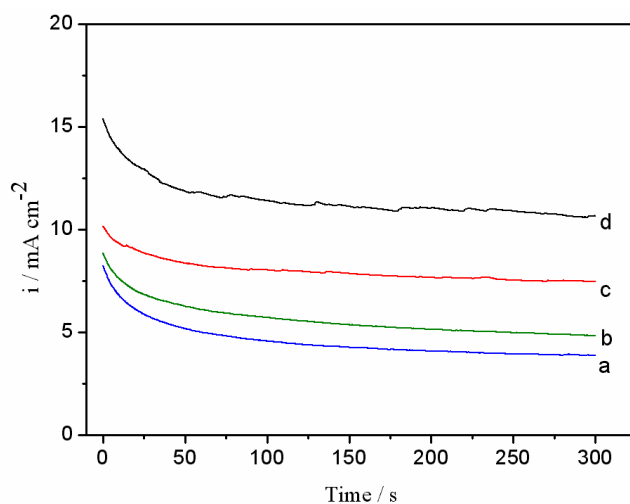


Figure 2. Amperometric i - t Curves of the coating electrodes in a 0.05 M Na₂SO₄ solution under 2.5 V. Ti/SnO₂-Sb (a) and Ti/SnO₂-Sb-Ce (b) without 500 mg L⁻¹ aniline. Ti/SnO₂-Sb (c) and Ti/SnO₂-Sb-Ce (d) with 500 mg L⁻¹ aniline

The electrochemical property of the two electrodes was studied through Amperometric i - t Curve. Fig. 2 shows the evolution of the current densities on the two electrodes under 2.5 V. It can be

seen that the current densities of the Ti/SnO₂-Sb and Ti/SnO₂-Sb-Ce electrodes are about 3.9 and 4.8 mA cm⁻² in a 0.05 M Na₂SO₄ solution without 500 mg L⁻¹ aniline, respectively. The current densities of the two electrodes are all increased after addition of aniline to the solution. On Ti/SnO₂-Sb, the current density increases to 7.4 mA cm⁻², and the current density increases to 10.7 mA cm⁻² on Ti/SnO₂-Sb-Ce. The increase of the current density can be attributed to the electrochemical oxidation of aniline on the electrodes. The current density increase on Ti/SnO₂-Sb-Ce is higher than that on Ti/SnO₂-Sb, and this could be partially attributed to an improvement of the oxidation of organic compounds by Ce doping.

3.2. Electrochemical oxidation

Two different electrodes have been compared as the anode in electrochemical degradation of aniline to further evaluate the effect of the Ce doping for electro-catalysis oxidation. As Fig. 3 showed, it can be noticed from the graph that the steep increase for aniline removals with Ti/SnO₂-Sb-Ce electrode was obtained in electrolysis reaction time of 1 h, and aniline removal was obviously faster on the Ti/SnO₂-Sb-Ce than that on the Ti/SnO₂-Sb electrode. The aniline removals are 98.3% and 82.7% for the two electrodes at reaction time of 2 h, respectively.

COD removals of aniline solution by the two electrodes were compared in electrochemical oxidation (Fig. 4). The COD was removed more rapidly on the Ti/SnO₂-Sb-Ce electrode than that on the Ti/SnO₂-Sb electrode.

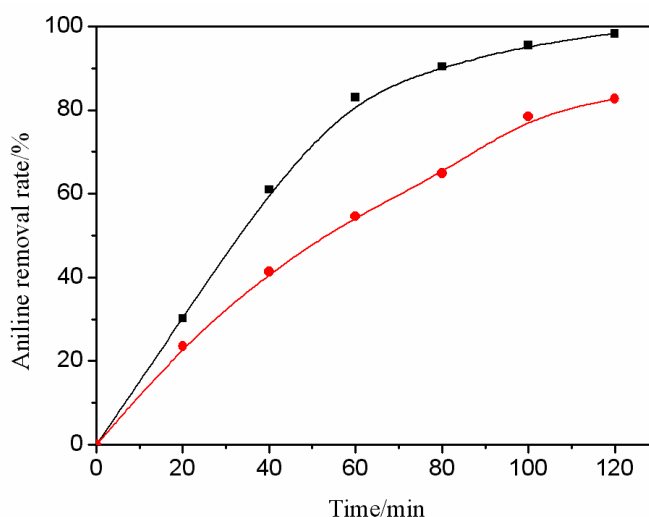


Figure 3. Comparison of aniline removal between (■) the Ti/SnO₂-Sb-Ce and (●) the Ti/SnO₂-Sb in 500 mg L⁻¹ aniline and 0.05 M Na₂SO₄ solution. Current density 30 mA cm⁻²

For two electrodes, 80.5 and 58.4% of COD removal were achieved in 2 h, respectively, which shows that organic compounds are more effectively oxidized on the Ti/SnO₂-Sb-Ce anode. Those are associated with oxidation of aniline into intermediate compounds, and then some intermediate

compounds were further converted to CO_2 and H_2O . The instantaneous current efficiency (ICE) of the electrolysis was calculated by the ICE equation. ICE on the two electrodes gradually decreased during electrolysis, but it was obviously higher on the Ti/SnO₂-Sb-Ce electrode than that on the Ti/SnO₂-Sb electrode. The ICEs are 36.5% and 26.5% at 2 h for the Ti/SnO₂-Sb-Ce and Ti/SnO₂-Sb electrodes, respectively. These results show that it is more efficient for aniline oxidation on the Ti/SnO₂-Sb-Ce electrode than that on the Ti/SnO₂-Sb electrode.

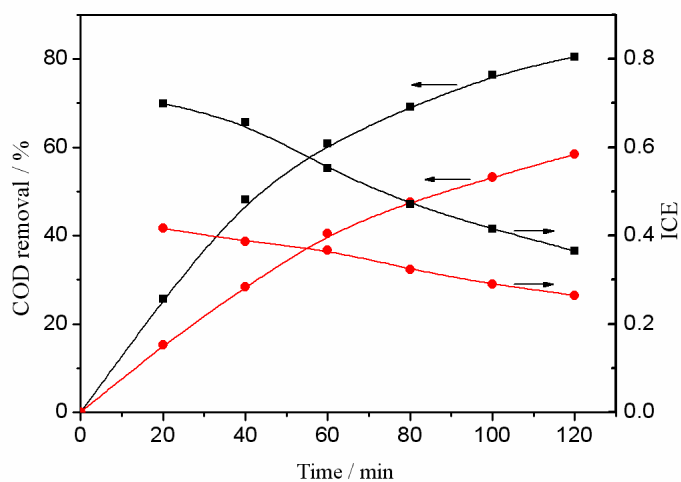


Figure 4. COD removal and ICE in 500 mg L⁻¹ aniline and 0.05 M Na₂SO₄ solution during electrolysis. Current density 30 mA cm⁻². (■) Ti/SnO₂-Sb-Ce, (●) Ti/SnO₂-Sb

3.3. Characterization of coating

Fig. 5 shows the SEM microstructures of the Ti/SnO₂-Sb-Ce and Ti/SnO₂-Sb electrodes. Nano-scale particles were found on the coating surface of the two electrodes.

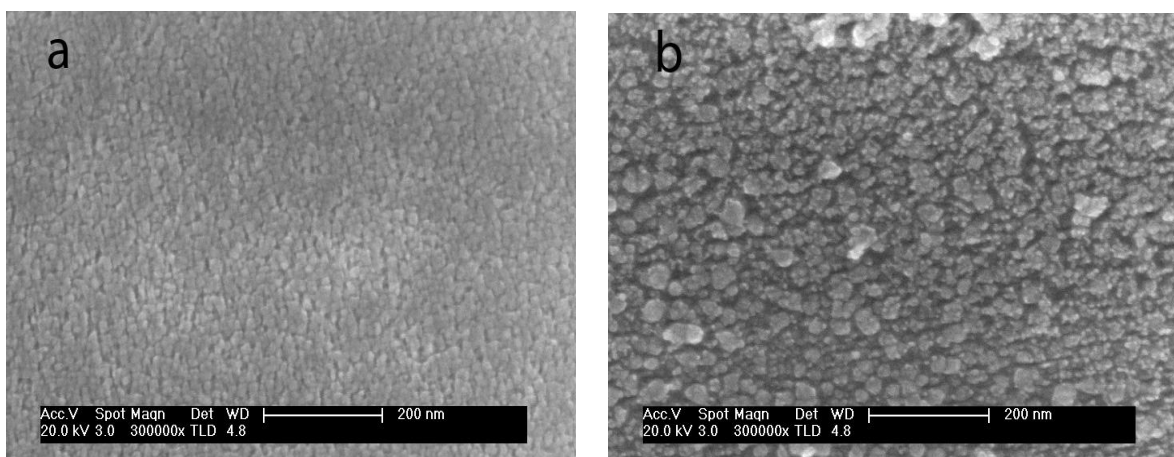


Figure 5. SEM surface images of the Ti/SnO₂-Sb-Ce electrode (a) and the Ti/SnO₂-Sb electrode (b)

Particle sizes of the Ti/SnO₂-Sb-Ce become smaller than that of the Ti/SnO₂-Sb due to Ce doping, and the coating particles of the Ti/SnO₂-Sb-Ce appeared to be more uniformly distributed. Particle sizes of the Ti/SnO₂-Sb-Ce and Ti/SnO₂-Sb electrodes are about 10-20 nm and 20-50 nm, respectively. The Ti/SnO₂-Sb-Ce electrode had larger surface areas and could provide with more active sites for electrochemical oxidation. EDS confirmed the presence of Sn, Sb and Ce in the Ce-doped electrode (Fig. 6).

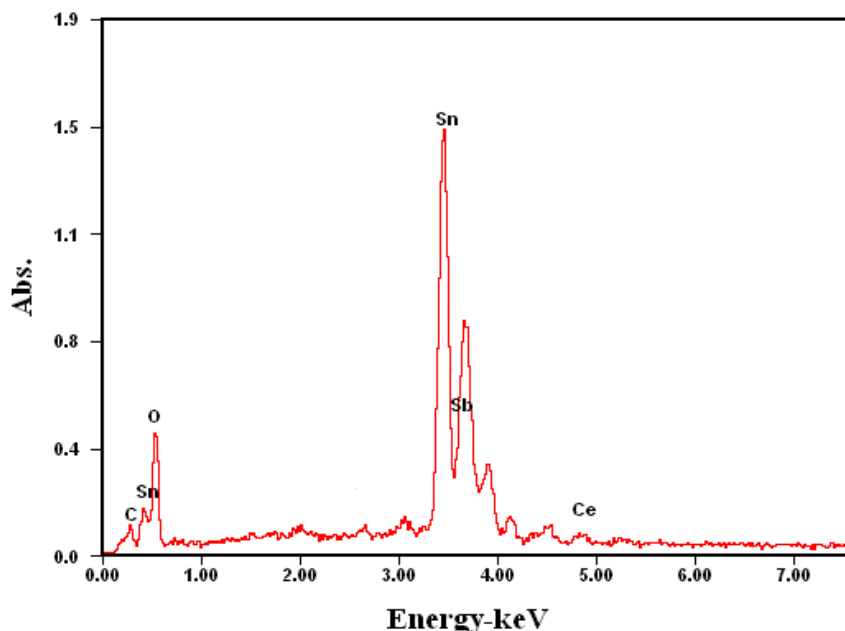


Figure 6. EDS of the Ti/SnO₂-Sb-Ce electrode

Fig. 7 records the XRD patterns of the Ti/SnO₂-Sb-Ce and the Ti/SnO₂-Sb, which only show a series of diffraction peaks of the SnO₂ structure and metal Ti substrate. The peaks corresponding to $2\theta \approx 26.7^\circ$, 33.8° and 51.9° were assigned to the (110), (101) and (211) planes of SnO₂. The peak positions agreed well with the reflections of SnO₂, indicating a tetragonal rutile structure. No diffraction peak of Ce and Sb metal oxides was clearly found from the XRD spectra, which indicates that the doping ions substituted for Sn⁴⁺ in the SnO₂ crystal lattice or Ce and Sb phases were particularly well-dispersed on the coatings [27]. The average crystallite size of SnO₂ was estimated using the Scherrer equation [28]. The average crystallite sizes of the (110) plane of SnO₂ were about 14.4 and 8.9 nm for the Ti/SnO₂-Sb and Ti/SnO₂-Sb-Ce, respectively. The decrease of the crystallite size can be ascribed as the growth of the crystal phase is hindered by the high distortion effects owing to Ce-doping in the lattice shape. Smaller crystallite sizes are favorable to improve electrochemical capability of the electrode.

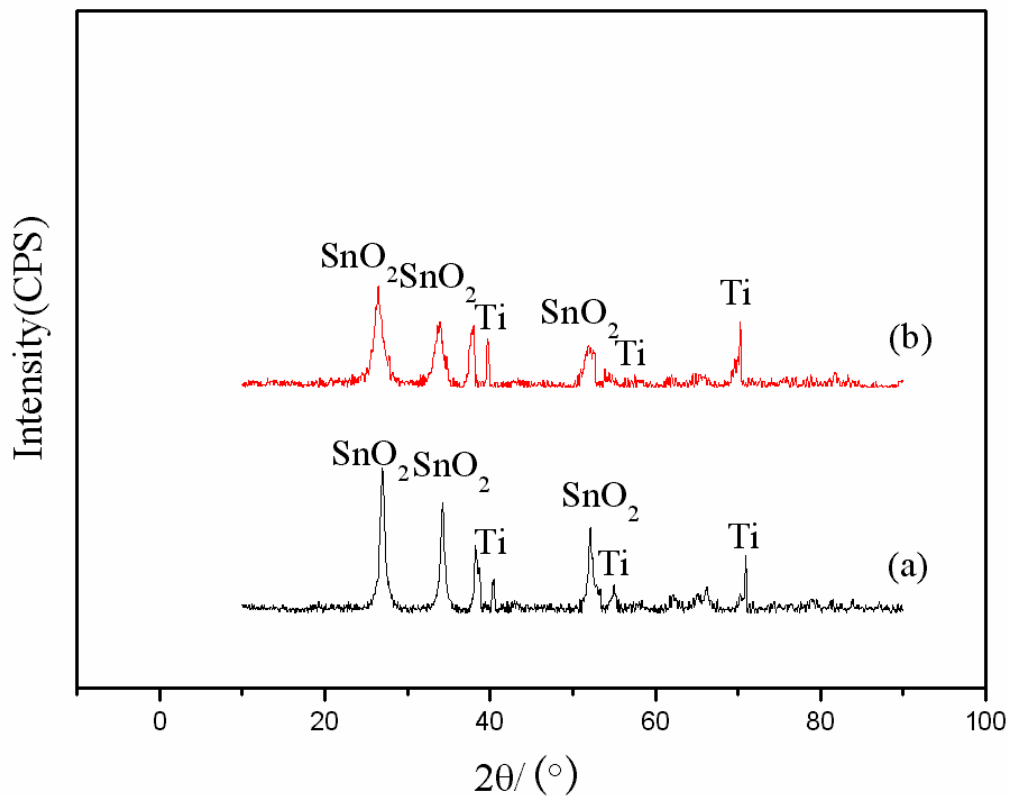


Figure 7. XRD patterns of the Ti/SnO₂-Sb electrode (a) and the Ti/SnO₂-Sb-Ce electrode (b)

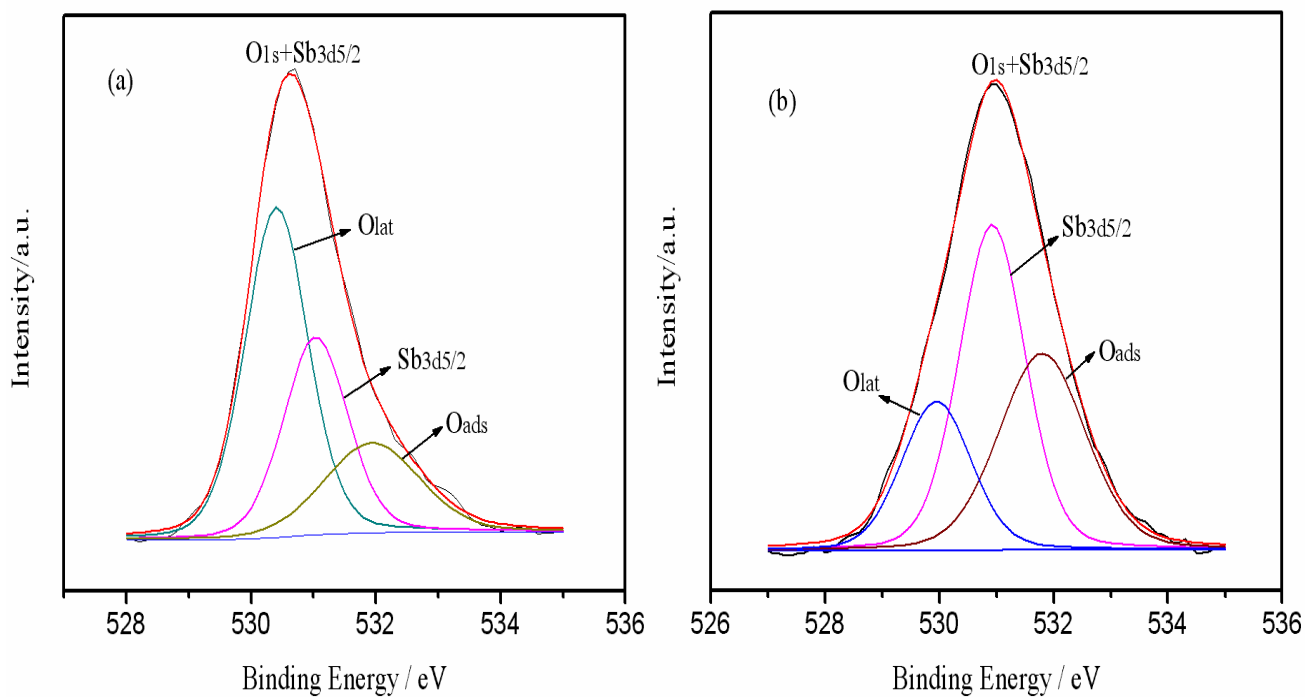
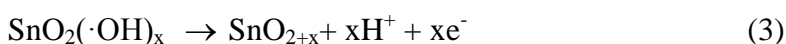
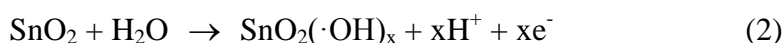


Figure 8. Fitted curves of O1s and Sb3d_{5/2} XPS spectra on the coating surfaces of the Ti/SnO₂-Sb (a) and Ti/SnO₂-Sb-Ce (b) electrodes

Table 1. XPS analysis of on the Surfaces of the Ti/SnO₂-Sb and Ti/SnO₂-Sb-Ce electrodes

sample	Binding energy[eV]				O _{ads} content[%]	O _{lat} content[%]
	Sn3d _{5/2}	Sb3d _{5/2}	O1s(ads)	O1s(lat)		
Ti/SnO ₂ -Sb	486.71	530.99	531.86	530.36	29.13	70.87
Ti/SnO ₂ -Sb-Ce	486.97	530.92	531.80	529.95	62.17	37.83

XPS was employed to study the surface composition and element chemical state of the coating. The XPS investigation was focused mainly on the detailed analysis of O elements. The XPS spectra of Sb3d_{5/2} and O1s are overlapped. They were fitted as shown in Fig. 8. The mixed spectra was fitted into three peaks, which correspond to different species, and the deconvoluted values are given in Table 1. The banding energy of Sb3d_{5/2} was around 531.0 eV for two electrodes, in agreement with other researchers for Sb⁵⁺ [29]. Two O1s peaks appeared after deconvolution. The lower binding energy peak (about 530 eV) is assigned to the lattice oxygen O_{lat} which are incorporated into SnO₂ crystal lattice, and the higher binding energy peak (about 532 eV) may be ascribed to adsorbed oxygen species O_{ads} which are adsorptive O₂ and/or weakly bonded oxygen species (e.g. hydroxyl group) [30,31]. The relative content of different kinds of oxygen species could be calculated by their XPS intensities and sensitivities. Table 1 shows content of different chemical states of the O element on the surface of the different electrodes. O_{ads} content is 62.17% for the Ti/SnO₂-Sb-Ce electrode and 29.13% for the Ti/SnO₂-Sb electrode. The O_{ads} is the most active oxygen species and plays an important role in oxidation process [32]. Electrochemical oxidation of organic pollutants can be detailed shown as below [33,34].



The oxidation of water molecule on the electrode surface gives rise to formation of physisorbed hydroxyl radicals (SnO₂(·OH)_x, O_{ads}). SnO₂(·OH)_x can oxidize the crystal lattice of SnO₂ to a higher state forming higher oxide SnO_{2+x}. The physisorbed hydroxyl radicals (SnO₂(·OH)_x), because of their high reactivity toward most organic compounds, are readily reacting with organic substrates close to anode surface to form carbon dioxide and water. RO represents the incomplete oxidation of organic compounds. O_{ads} contents on the surface of the Ti/SnO₂-Sb-Ce electrode were much higher than that on the Ti/SnO₂-Sb electrode. Therefore, complete oxidation of organic compounds (reaction 4) occurs

much more easily. Ce doping in SnO₂ coating enhanced the physisorbed capacity of •OH on electrode surface, which was beneficial to the electrochemical oxidation of organic compounds.

Electrochemical oxidation could proceed through several steps such as mass transport, adsorption and direct or indirect reaction at the anode surface. Direct or indirect reaction can be considered as electrochemical conversion and electrochemical combustion [35]. The active sites of the Ce doped Ti/SnO₂-Sb electrode increase, and the introduction of Ce strengthens the capacity of physical adsorption for hydroxyl radicals on the electrode surface. Those lead to a quantitative increase of physisorbed hydroxyl radicals on the Ti/SnO₂-Sb-Ce electrode surface. When organic compounds came close to electrode surface, oxidation reaction with adsorbed active radicals was easy to occur. Complete combustion is more on the surfaces of the Ce doped Ti/SnO₂-Sb electrode than that on the Ti/SnO₂-Sb electrode, and so the degradation of phenol is of higher efficiency on the Ti/SnO₂-Sb-Ce electrode than that on the Ti/SnO₂-Sb electrode.

4. CONCLUSION

Crystallite sizes of the coating became smaller on the Ti/SnO₂-Sb-Ce electrode than that on the Ti/SnO₂-Sb electrode, and so the electroactive surface area of the Ti/SnO₂-Sb-Ce was increased and accompanied by an improvement of electrochemical properties of the Ti/SnO₂-Sb-Ce electrode. Ce doped in the coating of the electrode enhanced the physical adsorption capacity of electrode surface for active oxygen species, which led to improved effectiveness on aniline mineralization. The rates of aniline elimination and COD removal were higher on the Ti/SnO₂-Sb-Ce electrode than that on the Ti/SnO₂-Sb electrode.

ACKNOWLEDGMENTS

This work was financially supported by Jiangsu Provincial Natural Science Foundation (BK2008195) and Research Program of huaiyin institute of technology (HGB0908).

References

1. C. Sáez, R. López-Vizcaíno, P. Cañizares and M.A. Rodrigo, *Ind. Eng. Chem. Res.*, 49 (2010) 9631.
2. M.A. Maluleke and V.M. Linkov, *Sep. Purif. Technol.*, 32 (2003) 377.
3. R. Levi, M. Milman, M.V. Landau, A. Brenner and M. Herskowitz, *Environ. Sci. Technol.*, 42 (2008) 5165.
4. S. Hammami, N. Oturan, N. Bellakhal, M. Dachraoui and A.M. Oturan, *J. Electroanal. Chem.*, 610 (2007) 75.
5. T.C. An, X.H. Zhu and Y. Xiong, *Chemosphere*, 46 (2002) 897.
6. J.Q. Li, L.Q. Li, L. Zheng, Y.Z. Xian and L.T. Jin, *Electrochim. Acta*, 51 (2006) 4942.
7. M. Panizza, M. Delucchi and G. Cerisola, *J. Appl. Electrochem.*, 35 (2005) 357.
8. Y. Xiong, C. He, H.T. Karlsson and X.H. Zhu, *Chemosphere*, 50 (2003) 131.
9. L. Szpyrkowicz, S.N. Kaul, R.N. Neti and S. Satyanarayan, *Water Res.*, 39 (2005) 1601.

10. P. Cañizares, J.A. Domínguez, M.A. Rodrigo, J. Villaseñor and J. Rodríguez, *Ind. Eng. Chem. Res.*, 38 (1999) 3779.
11. J.L.N. Xavier, E.Ortega, J.Z. Ferreira, A.M. Bernardes and V. Pérez-Herranz, *Int. J. Electrochem. Sci.*, 6 (2011) 622.
12. O. Simond and C. Comninellis, *Electrochim. Acta.*, 42 (1997) 2013.
13. M. Vuković, D. Marijan, D. Čukman, P. Pervan and M. Milun, *J. Mater. Sci.*, 34 (1999) 869.
14. G.H. Chen, X.M. Chen and P.L. Yue, *J. Phys. Chem. B*, 106 (2002) 4364.
15. H.C. Ma, C.P. Liu, J.H. Liao, Y. Su, X.Z. Xue and W. Xing, *J. Mol. Catal. A: Chem.*, 247 (2006) 7.
16. R.F. Yunus, Y.M. Zheng, K.G. N. Nanayakkara and J. P. Chen, *Ind. Eng. Chem. Res.*, 48 (2009) 7466.
17. P. Duverneuil, F. Maury, N. Pebere, F. Senocq and H. Vergnes, *Surf. Coat. Technol.*, 151-152 (2002) 9.
18. M. E. Makgae, C.C. Theron, W.J. Przybylowicz and A.M. Crouch, *Mater. Chem. Phys.*, 92 (2005) 559.
19. C.L.P.S. Zanta, P.A. Michaud, C. Comninellis, A.R.D. Andrade and J.F.C. Boodts, *J. Appl. Electrochem.*, 33 (2003) 1211.
20. C.R. Costa, C.M.R. Botta, E.L.G. Espindola and P. Olivi, *J. Hazard. Mater.*, 153 (2008) 616.
21. Y.H. Song, G. Wei and R.C. Xiong, *Electrochim. Acta*, 52 (2007) 7022.
22. Y.j. Feng, Y.H. Cui, B. Logan and Z.Q. Liu, *Chemosphere*, 70 (2008) 1629.
23. S.Y. Ai, M.N. Gao, W. Zhang, Q.J. Wang, Y.F. Xie and L.T. Jin, *Talanta*, 62 (2004) 445.
24. J. Iniesta, P.A. Michaud, M. Panizza, G. Cerisola, A. Aldaz and C. Comninellis, *Electrochim. Acta*, 46 (2001) 3573.
25. C.L.P.S. Zanta, A.R.D. Andrade and J.F.C. Boodts, *J. Appl. Electrochem.*, 30 (2000) 467.
26. D.T. Cestarolli and A.R.D. Andrade, *Electrochim. Acta*, 48 (2003) 4137.
27. N. Li, C. Descorme and M. Besson, *Appl. Catal. B: Environ.*, 76 (2007) 92
28. A. Weibel, R. Bouchet, F. Boulc'h and P. Knauth, *Chem. Mater.*, 17 (2005) 2378.
29. B. Correalozano, C. Comninellis and A.D. Battisti, *J. Electrochem. Soc.*, 143 (1996) 203.
30. B.M. Trost, C. Chan and G. Ruhter, *J. Am. Chem. Soc.*, 109 (1987) 3486.
31. K. Srinivas, M. Vithal, B. Sreedhar, M.M. Raja and P.V. Reddy, *J. Phys. Chem. C*, 113 (2009) 3543.
32. S. Yang, Y. Feng, J. Wan, W. Zhu and Z. Jiang, *Appl. Surf. Sci.*, 246 (2005) 222.
33. S. Fierro, T. Nagel, H. Baltruschat and C. Comninellis, *Electrochem. Commun.*, 9 (2007) 1969.
34. C. Mousty, G. Fóti, Ch. Comninellis and V. Reid, *Electrochim. Acta*, 45 (1999) 451.
35. S. Fierro, T. Nagel, H. Baltruschat and C. Comninellis, *Electrochem. Commun.*, 9 (2007) 1969.